



HAL
open science

Relation between plasmonic tip emission and electromagnetic enhancement evidenced in tip-enhanced Raman spectroscopy

J. Plathier, A. Merlen, A. Pignolet, A. Ruediger

► **To cite this version:**

J. Plathier, A. Merlen, A. Pignolet, A. Ruediger. Relation between plasmonic tip emission and electromagnetic enhancement evidenced in tip-enhanced Raman spectroscopy. *Journal of Raman Spectroscopy*, 2017, 48 (12), pp.1863-1870. 10.1002/jrs.5260 . hal-04653945

HAL Id: hal-04653945

<https://hal.science/hal-04653945v1>

Submitted on 19 Jul 2024

HAL is a multi-disciplinary open access archive for the deposit and dissemination of scientific research documents, whether they are published or not. The documents may come from teaching and research institutions in France or abroad, or from public or private research centers.

L'archive ouverte pluridisciplinaire **HAL**, est destinée au dépôt et à la diffusion de documents scientifiques de niveau recherche, publiés ou non, émanant des établissements d'enseignement et de recherche français ou étrangers, des laboratoires publics ou privés.

Relation between plasmonic tip emission and electromagnetic enhancement evidenced in Tip Enhanced Raman Spectroscopy

J. Plathier¹, A. Merlen^{2*†}, A. Pignolet¹, A. Ruediger^{1*}

1 Institut National de la Recherche Scientifique, Centre Énergie Matériaux Télécommunications, 1650, Boulevard Lionel-Boulet Varennes, Québec, J3X 1S2, Canada.

2 Institut Matériaux Microélectronique Nanoscience de Provence, IM2NP, UMR CNRS 7334, Aix Marseille Université, Université de Toulon, Site de l'Université de Toulon, 83957, La Garde Cedex, France.

* Corresponding authors: merlen@univ-tln.fr, ruediger@emt.inrs.ca

† Present address: *Institut Fresnel UMR 7249, Aix-Marseille Université, CNRS, Ecole Centrale Marseille, 13013 Marseille, France.*

Abstract: We report Tip Enhanced Raman spectroscopy (TERS) measurements of single wall carbon nanotubes deposited on a barium titanate substrate. The TERS mappings demonstrate that the evolution of the gold tip enhanced luminescence is strongly correlated with the intensity of the Raman modes from the SWNTs and the substrate. As the tip emission is directly related to the plasmonic properties of the nanoantenna at the apex of the tip, it is possible to compare the frequency and intensity of each vibrational mode with the electromagnetic enhancement model. We find a very good agreement between all these parameters confirming the essential role of the electromagnetic enhancement mechanism in surface enhanced spectroscopy.

Keywords: tip-enhanced Raman spectroscopy; localized surface plasmon resonance; Carbon Nanotubes; gold luminescence.

Introduction

Tip Enhanced Raman Spectroscopy (TERS)¹ offers a unique combination of the extreme sensitivity of Surface Enhanced Raman Spectroscopy (SERS)² and the high spatial resolution of scanning probe techniques. It has been developed at the end of the 90s^{3,4} and since then several studies have proven its high efficiency in the field of Molecular Analysis,⁵ Self-Assembled Monolayers,⁶ Surface Chemistry,^{7,8} Nanomaterials,^{9,10} Molecular Phase Boundaries,¹¹ etc.

TERS is still considered as a demanding technique and regardless of all its promise, breakthroughs to deploy its potential as an enabling technology are yet to be delivered. Its principle is based on a strong electromagnetic enhancement at the apex of a tip due to a localized, resonant surface plasmon scanned over the sample surface. The tip acts as a nanoantenna which produces an enhanced near-field from the incoming electromagnetic field (laser and scattered light from the sample) and radiates it in a far field signal. To get a tangible signal this enhancement must be sufficiently large to exceed the far field background, which can be achieved using plasmonic

nanoantennas. For this reason, almost all TERS tips are prepared with gold or silver. High spatial resolution Raman maps are obtained if the signal contains a major contribution from the enhanced field, which in particular requires a highly localized electromagnetic enhancement. As a consequence, highly efficient and reproducible tips are needed for further developments of TERS.

To improve the preparation of efficient tips, it is necessary to have a clear idea of the enhancement mechanisms involved in TERS. In SERS it is assumed that two distinct mechanisms are responsible for the final enhancement of the Raman signal: the electromagnetic (EM) enhancement and the chemical (CM) enhancement. The latter is based on a charge transfer between the nanoantenna and the sample.¹² In TERS, the chemical enhancement may occur, if the tip-to-sample distance is small enough, but is virtually uncontrollable for imaging. As a consequence, a direct contact between the tip and the sample and such enhancement are unsuitable for controlled optimization. It must be noticed that the relative contribution of both chemical and electromagnetic enhancement in TERS is still under debate.¹³

Our study offers the opportunity to improve the preparation of TERS tips by a systematic comparison between the intensity of the TERS signal and the tip optical response. Several numerical simulations have already demonstrated the best configuration to achieve high electromagnetic enhancements.^{14–17} The role of polarization, tip-to-surface distance, excitation wavelength, *etc.*, is clearly evidenced in these studies. However few experimental studies have related the optical properties of the tip and the final enhancement for a simple experimental reason: it is extremely difficult to measure both the Raman signal and the optical response of the tip. Neascu *et al.* have proposed a method based on the spectral analysis of the light scattered by the tip, frustrating the evanescent light field produced by total internal reflection.¹⁸ This method has been applied to TERS by Methani *et al.*¹⁹ and a good qualitative agreement was found between the TERS spectra and the optical resonance of the tip. Nevertheless this technique has a major drawback: tip properties are measured with a prism and cannot be done *in situ* if the sample is non-transparent, which is commonly the case in TERS studies. In addition, numerical simulations have clearly demonstrated that the refractive index of the substrate needs to be taken into consideration for the optical properties of the coupled system of tip, sample and substrate for its optical response. In other words, responses measured by the prism will be strongly modified if the same tip is above a different surface. We present an *in situ* method for the determination of the tip optical properties directly associated with the TERS measurement.

We exploit the enhanced tip luminescence signal observed in our TERS spectra as a tool to determine the optical response of the tip. This response is compared with the intensity of the TERS modes of carbon nanotubes on a barium titanate substrate. Our results clearly confirm that the electromagnetic enhancement is the dominant mechanism in TERS and pave the way for a systematic and efficient analysis of TERS tips and their electromagnetic enhancement mechanism.

Method

Our experimental setup has been described in a previous publication.²⁰ Basically we performed TERS measurements with homemade etched gold tips with a 632.8 nm laser excitation. The typical optical resonance of such tips reported in the literature is located between 600 and 800 nm,^{21,22} which is in good agreement with our laser excitation. The tip is approached to the surface using a tuning fork based atomic force microscope in shear force configuration. We have performed TERS mapping with a typical acquisition time for each spectrum of 1 s.

Metallic Single Wall Carbon Nanotubes (SWNT) in aqueous solution have been purchased at Nanointegris[®].²³ The provider indicates a mean diameter of 1.4 nm. They have been drop-cast on a barium titanate (BaTiO₃) monocrystal (MaTeck GmbH). After drying under ambient conditions, excess chemicals were rinsed with DI water.

In our recorded TERS spectra different contributions are present: the Raman modes originating from the barium titanate substrate (mainly from the far-field signal), the carbon nanotubes (mainly from the near-field signal) and the optical emission coming from the tip itself²⁴ (from near-field signal). All these contributions have been carefully deconvoluted using a homemade software code. First, the carbon nanotube contribution was isolated by subtracting the signal of barium titanate and tip emission taken right next to the nanotube. Then, the tip emission was isolated by subtracting a barium titanate far field spectrum taken at the exact same position with the tip retracted. Finally, each contribution was numerically fitted using symmetric and asymmetric Lorentzian^{25,26} line shapes. In order to check the result, a fit of the original TERS spectrum was made using the result of the deconvolution and compared to the latter. The fit residue was also analyzed in every case to ensure that every mode was taken into account.

Results and Discussion

A typical TERS signal of a carbon nanotube, as depicted in Figure. 1(a), was compared to the confocal Raman spectrum of both carbon nanotubes [Figure. 1(b)] and barium titanate [Figure. 1(c)]. In the TERS spectrum four modes, from BaTiO₃ [A₁(TO₂) at 276 cm⁻¹, E(TO₃) at 305 cm⁻¹, A₁(TO₃) at 520 cm⁻¹ and A₁(LO₃) at 710 cm⁻¹] substrate, are observed.^{27,28} The main features of SWNT Raman modes are also clearly visible:²⁹

- The Radial Breathing Modes (RBM) at 172 cm⁻¹. It corresponds to the typical value expected for metallic nanotubes with a diameter of 1.4 nm;³⁰
- The defect mode (D) at 1320 cm⁻¹;
- The graphite modes (G) between 1550 cm⁻¹ and 1580 cm⁻¹.

These modes are intense and have been extensively studied for SWNT.^{9,31,32} Their analysis indicate the tube diameter (RBM), structural defects (D modes), chirality, etc. It can be observed in Figure. 1 that weaker modes are also visible, notably the oTO mode at 860 cm⁻¹ and the M mode at 1755 cm⁻¹. The oTO mode is usually observed

in IR spectrum of SWNT.³³ It is associated with a first order zone center vibrational mode. The M mode is an overtone of the oTO.³⁰ An enhancement for the G mode by a factor 1000 is observed. The local electric field enhancement of the tip is then estimated around 20 by correcting the intensity ratio between the near-field signal and the far field signal by the area excited by each fields.³⁴ In addition to these Raman modes, a broad optical emission coming from the gold tip is visible and isolated by the deconvolution of the spectrum [Figure. 1(d)]. This type of emission has already been reported^{35,36}, and is assumed to be the gold photoluminescence³⁷ amplified by the localized surface plasmon resonance (LSPR) at the apex of the tip. Recently Lin *et al.*³⁸ have reported a direct correlation, supporting this assumption, between this plasmon enhanced luminescence and the SERS signal intensity on single gold nanorods. Considering a simple model independent of the physical mechanism involved in the luminescence, they have suggested that this emission is an intrinsic fingerprint of the plasmonic spectral response of the nanostructure.

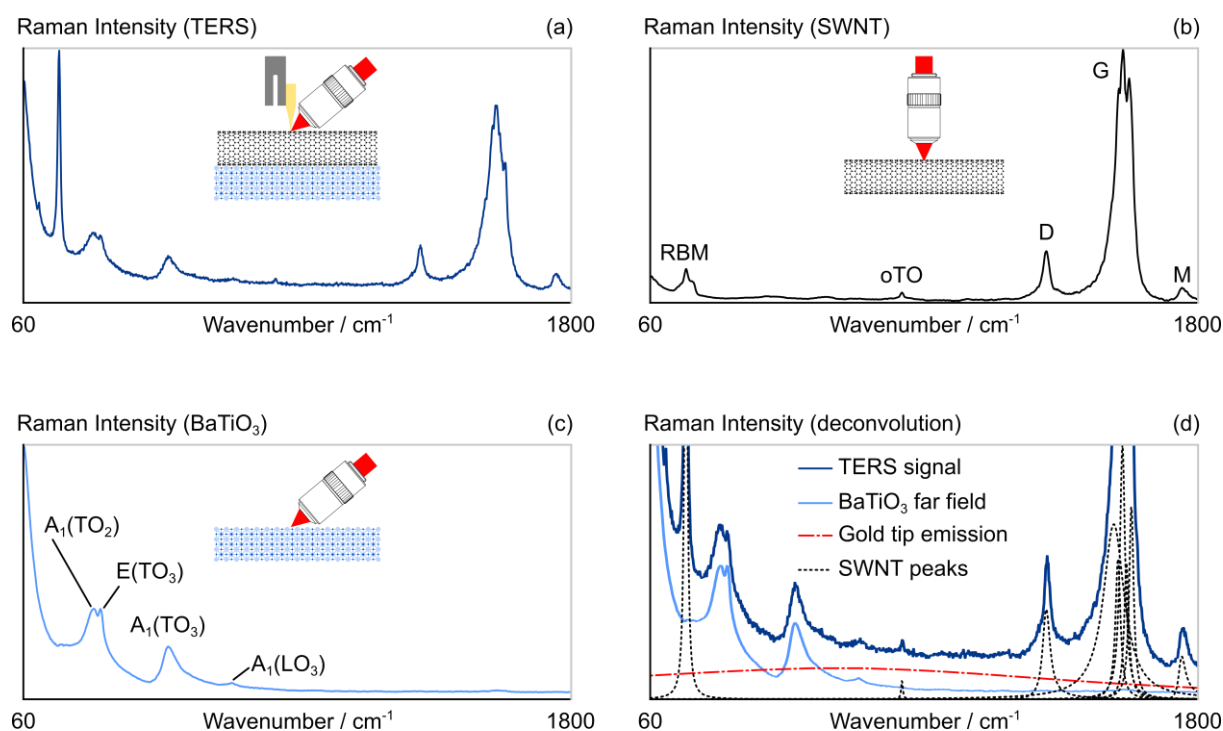


Figure. 1. The TERS spectrum of a carbon nanotube deposited on a barium titanate crystal (a) contains the far-field and the near-field contribution of carbon nanotubes (b) and barium titanate (c). Spectra shown in (b) and (c) are the far-field reference for carbon nanotubes and the barium titanate substrate respectively. The deconvolution (d) of the contributions of both carbon nanotubes (dotted black) and barium titanate (light blue) spectra in the TERS signal reveals the underlying enhanced gold luminescence of the tip (dash-dotted red). Schemes show the experimental configuration used to acquire each spectrum.

To study the influence of the electromagnetic interaction and to limit thermal drift, we have chosen rather fast TERS maps (typically 15 min for a complete scan). At such a scan speed the tip undergoes moderate alterations during the mapping, in particular

due to the ductility of gold and the interactions between the tip and the sample. Deformations of the tip shape can be indirectly followed through the evolution of the frequency of its enhanced luminescence, which is progressively red shifted during the scan, as it can be seen in Figure 2(a) and 2(b). At the lower part of Figure 2(a), the resonance is centered at lower wavenumber compared to the upper part. This is the evidence of the degradation of the tip, expressed by an increasing radius, as optical properties of nanoantenna are extremely sensitive to their shape. In our case, it offers the opportunity to carefully study the evolution of the Raman signal related to the optical response of the tip.

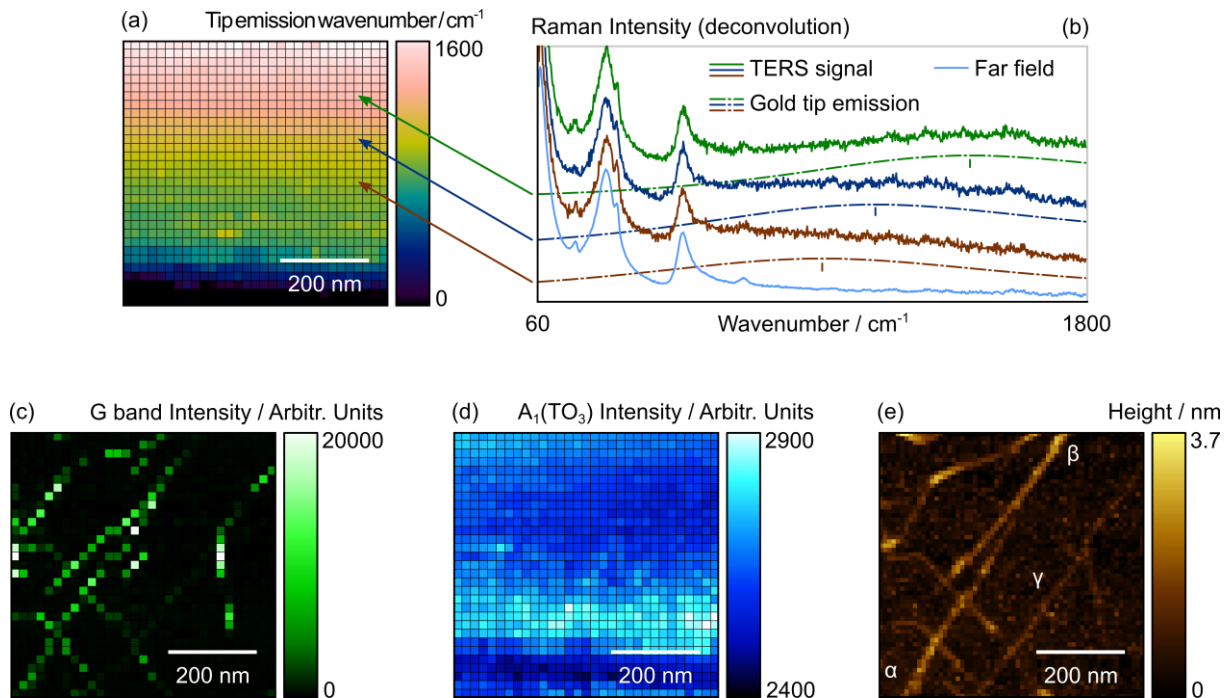


Figure 2. (a) Mapping of the gold tip enhanced luminescence wavenumber (31×31 pixels, pixel size: $20 \text{ nm} \times 20 \text{ nm}$). (b) Typical optical spectra for different places of the mapping. The tip emission obtained after data processing (notably its position as shown in (a)) is evidenced by the dash-dotted lines. TERS Mapping of the intensity of G modes of carbon nanotubes (c) and the intensity of the A_1 mode from the barium titanate substrate (d). The corresponding topography image (e) attests the high spatial resolution of the TERS mapping. Maps were recorded from the bottom-left corner to the top-right corner with a horizontal fast axis.

The high spatial resolution of the TERS mapping (SWNT clearly visible in Figure 2(c) with an apparent width below 20 nm) confirms that we are performing optical near-field measurements. In addition, it can be seen in Figure 2(c) and 2(d) that the intensity of Raman modes from both SWNT and BaTiO_3 is not homogenous over the whole image: clearly, some specific regions exhibit higher intensity. We can exclude a coincidental distribution of resonant SWNT in the middle of the scanned area taking into consideration the intensity of the G mode [Figure 2(c)] of the nanotubes labeled α , β and γ in Figure 2(e). If the variations in the G band intensity were only related to the

resonance of SWNT, the intensity would be expected to remain constant along each nanotube. In the present case we observe that the intensity of the G band along α and β reaches a maximum in the middle of the map while the intensity of γ start to increase only at the top of the map.

Noticing that the enhanced luminescence from the tip also evolved during the mapping process, we investigate the emission position, being depicted in Figure 2(a) and 2(b). Figure 2(a), 2(c) and 2(d), show that barium titanate modes are clearly more intense at the bottom of the figure, where the enhanced luminescence position is located at low wavenumbers, whereas the G modes are more intense in the middle and upper part, where the enhanced luminescence is located at higher wavenumbers. We attribute this variation in Raman modes intensity to a red shift of the LSPR frequency, reflected by the position of the tip enhanced luminescence, visible by comparing Figure 2(a), 2(c) and 2(d). The region where the barium titanate $A_1(TO_3)$ mode is more intense corresponds to a tip enhanced luminescence centered at low wavenumber (typically lower than 1000 cm^{-1}) whereas the one corresponding to intense G band intensity is associated with a tip emission at high wavenumber (typically higher than 800 cm^{-1}).

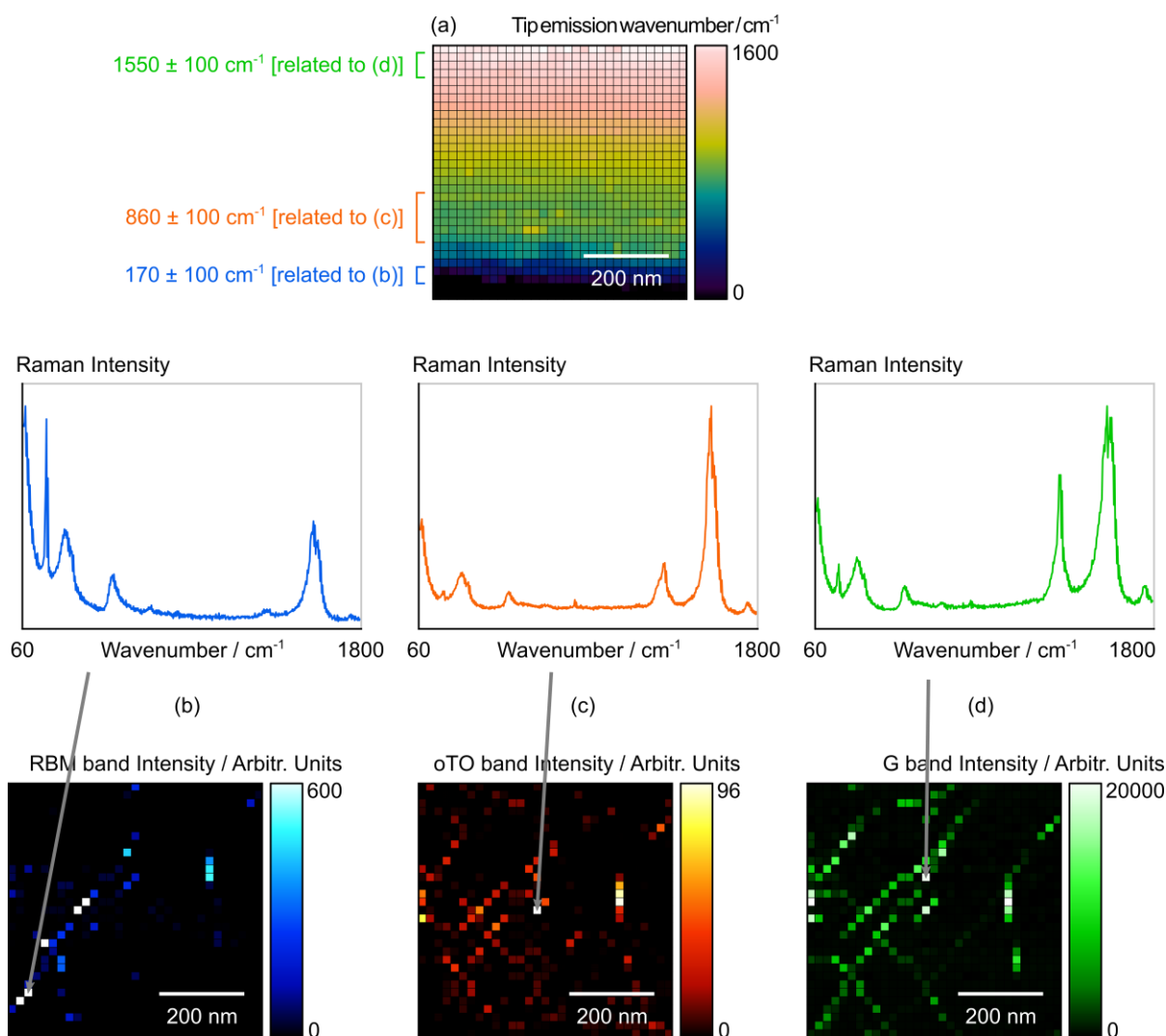


Figure 3. (a) Tip emission wavenumber mapping (as described in figure 2 (a)). TERS mapping of the enhanced intensities of RBM (a), oTO (b) and G-band (c) modes of SWNT. Areas for which the gold tip emission position is in the same spectral range as each Raman modes of SWNT are evidenced in (a). For each Raman mode the enhanced intensity in TERS mappings is directly correlated to the position of tip emission.

To confirm this hypothesis we have related the intensities maps of three modes of the SWNT (RBM, oTO and G modes) to the position of the tip enhanced luminescence, as presented in Figure. 3. We have not reported the D mode as its intensity is related to defects in SWNT structure and can thus vary independently of the tip enhancement. The interested reader can find it in supplementary information. Again, it is confirmed that Raman intensity and wavenumber of tip emission are directly related: The RBM is more intense at the lower part, at the beginning of the scan, the oTO mode in the middle and G band in the upper part, toward the end of the scan. This appears more drastically if we compare Raman spectra recorded in the lower and upper part of the mapping: the intensity of the RBM mode related to the G band is much higher in the lower part. Once again this feature can be related to the tip emission frequency: Raman

modes are more intense when the enhanced luminescence occurs at wavenumbers close to their own frequency. This result confirms that the enhanced luminescence is related to the LSPR frequency of the tip in accordance with the model proposed by Lin et al.³⁸: an optical resonance of the tip close to the Raman modes will ensure a high electromagnetic enhancement giving rise to intense Raman modes. This is a direct experimental evidence of the electromagnetic enhancement in TERS measurements. It also evidences another challenge for the preparation of highly efficient TERS tips: the final electromagnetic enhancement is extremely dependent on its shape and will only apply to a limited spectral range. Even a slight change in the enhanced luminescence frequency, such as observed during our scan will affect the optical efficiency of the tip associated with a dramatic decrease in the TERS signal intensity. With the technology commonly used nowadays for the preparation of TERS tips it is virtually impossible to have a perfect control and a high reproducibility in the position of the surface plasmon resonance.

To go further in the analysis of the enhancement mechanism in our TERS measurement we have reported TERS mapping for three modes of SWNT in comparison with the position of the tip emission in Figure. 3. If we compare these figures carefully, it appears that intense Raman modes are not observed for the tip enhanced luminescence occurring exactly at the same frequency. This is clearly visible in particular for the G modes: its intensity is high in the middle and higher part of the figure for a corresponding emission higher than 600 cm⁻¹, which is very far from the position of this mode. This feature can be explained by the physical enhancement mechanism of enhanced spectroscopy. Raman scattering is an inelastic process involving two photons with slightly different frequencies. Thus the EM enhancement occurs for both the excitation and scattering wavelengths according to the formula of the enhancement factor (EF):

$$EF \propto g^2(\omega_e)g^2(\omega_R).$$

Where $g(\omega_e)$ is the local electric field enhancement at the laser frequency and $g(\omega_R)$ the field enhancement at the scattering frequency. Usually for most studies the difference between the excitation and scattering wavelengths is negligible, in particular in SERS for which the large number of nanoantennas ensure a very broad SPR. In such conditions the relation between excitation wavelength, optical resonance and final enhancement has already been studied.³⁹ In TERS, a single nanoantenna is used and as previously demonstrated the Raman signal is strongly affected by any change in its resonance. In addition, to get a significant enhancement, this resonance should occur between the excitation and scattering wavelengths, ensuring a good compromise between the amplification of $g(\omega_e)$ and $g(\omega_R)$. For low frequency modes the difference between ω_e and ω_R is negligible. This is the reason why RBM modes have the highest observed signal for tip's surface plasmon resonance frequencies close to the mode position [which corresponds to the lower part of Figure. 3(b)]. For the G modes, this difference is no longer negligible, and stronger enhancement is expected for LSPR frequencies centered between excitation and Raman scattering. This is why in

Figure. 3(d), the highest intensity is observed for this mode at wavenumbers lower than 1550 cm^{-1} . Once again this result confirms the model of the electromagnetic enhancement in TERS. It also suggests an important limitation of TERS: a significant enhancement requires a resonance for both excitation and scattering frequencies. This imposes severe conditions to tips for the enhancement of high frequency modes (typically having a wavenumber higher than 3000 cm^{-1}) for which the difference between ω_e and ω_R is larger than a typical plasmon resonance.

As a first conclusion, the study of both the enhanced luminescence of the tip and Raman modes from SWNT has evidenced the electromagnetic enhancement in TERS. To confirm if this result depends on the sample, we have carefully studied the signal coming from the barium titanate substrate. TERS has already been reported on individual barium titanate nanocrystals⁴⁰ but in our case we tried to perform similar measurements on a bulk substrate, which is a big experimental challenge as it is hardly possible to discriminate between the near-field signal and far field background for TERS on a low-absorption bulk substrate. The signal comprises contributions from the confocal volume and from the much smaller, but tip-enhanced volume as sketched in Figure. 4(a). The ratio between these two contributions (typically $10^3\text{ nm}^3/1\text{ }\mu\text{m}^3 = 10^{-6}$) is so low that only extremely high electromagnetic enhancement may discriminate the near field against the background. For this reason, most TERS studies are performed on isolated nanostructures (such as nanotubes) or molecular monolayers on highly absorbing or reflecting substrates.

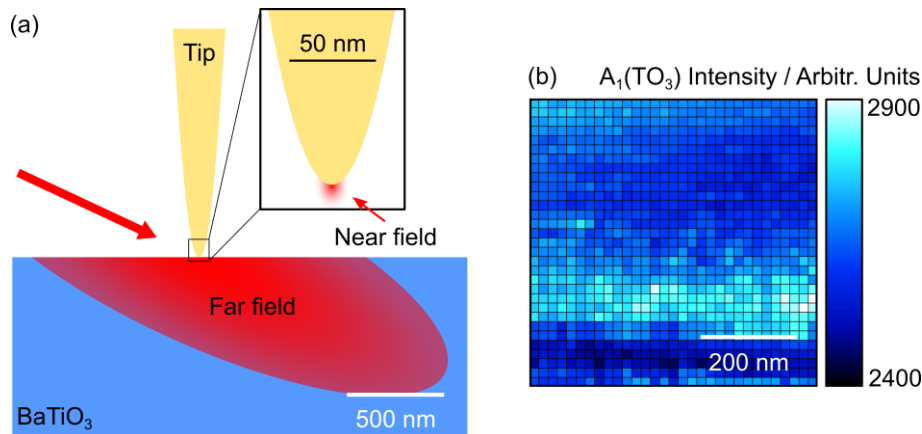


Figure. 4. (a) Scheme representing the volumes of interaction of the near field and the far field with the substrate. (b) Barium titanate $A_1(\text{TO}_3)$ mode intensity showing a weak amplification for a tip enhanced luminescence position between 640 cm^{-1} and 1000 cm^{-1} .

The signal recorded on barium titanate is reported in Figure. 4(b) ($A_1(\text{TO}_3)$ mode at 520 cm^{-1}). As mentioned above, it appears that the barium titanate signal is not homogenous over the whole surface: it is slightly but clearly higher in a specific part of the image. Once again it can be related to the physical mechanism in TERS: the Raman modes of barium titanate are enhanced for parts of the image with the plasmon resonance close to the respective frequencies. This result proves two main features:

first, it is possible to perform TERS on bulk substrates but the relative contribution of the near-field signal compared with the far field background is low, secondly, the electromagnetic enhancement mechanism is independent of the sample.

Conclusion

The electric field enhancement in apertureless optical nearfield microscopy, generated by a localized surface plasmon resonance at the apex of a gold tip, provides a spectrally confined amplification that has been successfully used for tip-enhanced Raman spectroscopy throughout recent years. Here, we demonstrate that modifications of the tip-shape, intentional or unintentional during scans, have an immediate impact on the spectral position of the surface plasmon resonance that we monitor through the enhanced luminescence from the tip itself. The enhancement of the luminescence correlates well with the enhancement of the Raman signal considering that the surface plasmon resonance is required to enhance both the excitation as well as the signal wavelength to achieve the g^4 amplification in Raman intensity. For Raman spectra extending over a relatively large spectral range, typical tips will therefore not be able to provide wavenumber-independent amplification and might not provide detectable amplification at all for wavenumbers beyond 3000 cm^{-1} .

Acknowledgements

A.R. is grateful for an NSERC discovery grant RGPIN-2014-05024.

References

- (1) Langelüdecke, L.; Singh, P.; Deckert, V. Exploring the Nanoscale: Fifteen Years of Tip-Enhanced Raman Spectroscopy. *Appl. Spectrosc.* **2015**, *69*, 1357–1371.
- (2) Etchegoin, P. G.; Le Ru, E. C. *Principles of Surface-Enhanced Raman Spectroscopy and Related Plasmonic Effects*; Elsevier, 2009.
- (3) Stockle, R. M.; Suh, Y. D.; Deckert, V.; Zenobi, R. Nanoscale Chemical Analysis by Tip-Enhanced Raman Spectroscopy. *Chem. Phys. Lett.* **2000**, *318*, 131.
- (4) Hayazawa, N.; Inouye, Y.; Sekkat, Z.; Kawata, S. Metallized Tip Amplification of near-Field Raman Scattering. *Opt. Commun.* **2000**, *183*, 333.
- (5) Zhang, R.; Zhang, Y.; Dong, Z. C.; Jiang, S.; Zhang, C.; Chen, L. G.; Zhang, L.; Liao, Y.; Aizpurua, J.; Yang, J. L.; *et al.* Chemical Mapping of a Single Molecule by Plasmon-Enhanced Raman Scattering. *Nature* **2013**, *498*, 82.
- (6) Horimoto, N. N.; Tomizawa, S.; Fujita, Y.; Kajimoto, S.; Fukumura, H. Nano-Scale Characterization of Binary Self-Assembled Monolayers under an Ambient Condition with STM and TERS. *Chem. Commun.* **2014**, *50*, 9862.
- (7) Sun, M.; Fang, Y.; Zhang, Z.; Xu, H. Activated Vibrational Modes and Fermi Resonance in Tip-Enhanced Raman Spectroscopy. *Phys. Rev. E. Stat. Nonlin. Soft Matter Phys.* **2013**, *87*, 20401.

- (8) Merlen, A.; Chaigneau, M.; Coussan, S. Vibrational Modes of Aminothiophenol: A TERS and DFT Study. *Phys. Chem. Chem. Phys.* **2015**, *17*, 19134–19138.
- (9) Cançado, L. G.; Hartschuh, A.; Novotny, L. Tip-Enhanced Raman Spectroscopy of Carbon Nanotubes. *J. Raman Spectrosc.* **2009**, *40*, 1420–1426.
- (10) Chanchaiyakul, S.; Yano, T.; Khoklang, K.; Krukowski, P.; Akai-Kasaya, M.; Saito, A.; Kuwahara, Y. Nanoscale Analysis of Multiwalled Carbon Nanotube by Tip-Enhanced Raman Spectroscopy. *Carbon N. Y.* **2016**, *99*, 642–648.
- (11) Jiang, N.; Chiang, N.; Madison, L. R.; Pozzi, E. A.; Wasielewski, M. R.; Seideman, T.; Ratner, M. A.; Hersam, M. C.; Schatz, G. C.; Van Duyne, R. P. Nanoscale Chemical Imaging of a Dynamic Molecular Phase Boundary with Ultrahigh Vacuum Tip-Enhanced Raman Spectroscopy. *Nano Lett.* **2016**, *16*, 3898–3904.
- (12) Sun, M.; Liu, S.; Chen, M.; Xu, H. Direct Visual Evidence for the Chemical Mechanism of Surface-Enhanced Resonance Raman Scattering via Charge Transfer. *J. Raman Spectrosc.* **2009**, *40*, 137–143.
- (13) Xia, L.; Chen, M.; Zhao, X.; Zhang, Z.; Xia, J. Visualized Method of Chemical Enhancement Mechanism on SERS and TERS. *J. raman Spectrosc.* **2014**, *45*, 533–540.
- (14) Kazemi-Zanjani, N.; Vedraïne, S.; Lagugne-Labarthe, F. Localized Enhancement of Electric Field in Tip-Enhanced Raman Spectroscopy Using Radially and Linearly Polarized Light. *Opt. Express* **2013**, *21*, 25271–25276.
- (15) Yang, Z.; Xu, H. Electromagnetic Field Enhancement in TERS Configurations. *J. Raman Spectrosc.* **2009**, *40*, 1343–1348.
- (16) Demming, A. L.; Festy, F.; Richards, D. Plasmon Resonances on Metal Tips : Understanding Tip-Enhanced Raman Scattering. *J. Chem. Phys.* **2005**, *122*, 184716.
- (17) Behr, N.; Raschke, M. B. Optical Antenna Properties of Scanning Probe Tips: Plasmonic Light Scattering, Tip-Sample Coupling, and Near-Field Enhancement. *J. Phys. Chem. C* **2008**, *112*, 3766–3773.
- (18) Raschke, M. B. Plasmonic Light Scattering from Nanoscopic. *Appl. Phys. B Lasers Opt.* **2005**, *80*, 295–300.
- (19) Mehtani, D.; Lee, N.; Hartschuh, R. D.; Kisliuk, A.; Foster, M. D.; Tsukerman, I. Optical Properties and Enhancement Factors of the Tips for Apertureless near-Field Optics. *J. Opt. A Pure Appl. Opt.* **2006**, *8*, S183–S190.
- (20) Merlen, A.; Plathier, J.; Ruediger, A. A near Field Optical Image of a Gold Surface: A Luminescence Study. *Phys. Chem. Chem. Phys.* **2015**, *17*, 21176–21181.
- (21) Mehtani, D.; Lee, N.; Hartschuh, R. D.; Kisliuk, A.; M D Foster; Sokolov, A. P.; Cajko, F.; Tsukerman, I. Optical Properties and Enhancement Factors of the Tips for Apertureless near-Field Optics. *J. Opt. A Pure Appl. Opt.* **2006**, *8*, S183–S190.

- (22) Sanders, A.; Bowman, R. W.; Zhang, L.; Turek, V.; Sigle, D. O.; Lombardi, A.; Weller, L.; Sanders, A.; Bowman, R. W.; Zhang, L.; *et al.* Understanding the Plasmonics of Nanostructured Atomic Force Microscopy Tips. *Appl. Phys. Lett.* **2016**, *109*, 153110.
- (23) <http://www.nanointegris.com/>.
- (24) Zheng, J.; Zhou, C.; Yu, M.; Liu, J. Different Sized Luminescent Gold Nanoparticles. *Nanoscale* **2012**, *4*, 4073.
- (25) Stancik, A. L.; Brauns, E. B. A Simple Asymmetric Lineshape for Fitting Infrared Absorption Spectra. *Vib. Spectrosc.* **2008**, *47*, 66–69.
- (26) Djemour, R.; Redinger, A.; Mousel, M.; Gütay, L.; Fontané, X.; Izquierdo-roca, V.; Pérez-rodríguez, A.; Siebentritt, S. The Three A Symmetry Raman Modes of Kesterite in Cu₂ZnSnSe₄. *Opt. Express* **2013**, *21*, 695–703.
- (27) Pezzotti, G.; Okai, K.; Zhu, W. Stress Tensor Dependence of the Polarized Raman Spectrum of Tetragonal Barium Titanate. *J. Appl. Phys.* **2012**, *111*, 13504.
- (28) Sendova, M.; Hosterman, B. D.; Raud, R.; Hartmann, T.; Koury, D. Temperature-Dependent, Micro-Raman Spectroscopic Study of Barium Titanate Nanoparticles. *J. Raman Spectrosc.* **2015**, *46*, 25–31.
- (29) Rao, A.M.; Richter, E.; Bandow, S.; Chase, B.; Eklund, P.C.; Williams, K.A.; Fang, S.; Subbaswamy, K.R.; Menon, M.; Thess, A.; Smalley, R.E.; Dresselhaus, G.; Dresselhaus, M. S. Diameter-Selective Raman Scattering from Vibrational Modes in Carbon Nanotubes. *Science (80-)*. **1997**, *275*, 187–191.
- (30) Jorio, A.; Saito, R.; Hafner, J. H.; Lieber, C. M.; Hunter, M.; McClure, T.; Dresselhaus, G.; Dresselhaus, M. S. Structural (N, M) Determination of Isolated Single-Wall Carbon Nanotubes by Resonant Raman Scattering. *Phys. Rev. Lett.* **2001**, *86*, 1118–1121.
- (31) Cançado, L. G.; Jorio, A.; Ismach, A.; Joselevich, E.; Hartschuh, A.; Novotny, L. Mechanism of Near-Field Raman Enhancement in One-Dimensional Systems. *Phys. Rev. Lett.* **2009**, *103*, 186101.
- (32) Dresselhaus, M. S.; Dresselhaus, G.; Saito, R.; Jorio, A. Raman Spectroscopy of Carbon Nanotubes. *Phys. Rep.* **2005**, *409*, 47.
- (33) Sbai, K.; Rahmani, a; Chadli, H.; Bantignies, J.-L.; Hermet, P.; Sauvajol, J.-L. Infrared Spectroscopy of Single-Walled Carbon Nanotubes. *J. Phys. Chem. B* **2006**, *110*, 12388–12393.
- (34) Kharintsev, S. S.; Hoffmann, G. G.; Fishman, A. I.; Salakhov, M. K. Plasmonic Optical Antenna Design for Performing Tip-Enhanced Raman. *J. Phys. D-Applied Phys.* **2013**, *46*, 145501.
- (35) Dulkeith, E.; Niedereichholz, T.; Klar, T. A.; Feldmann, J.; von Plessen, G.; Gittins, D. I.; Mayya, K. S.; Caruso, F. Plasmon Emission in Photoexcited Gold Nanoparticles. *Phys. Rev. B* **2004**, *70*, 205424.

- (36) Pettinger, B.; Domke, K. F.; Zhang, D.; Picardi, G.; Schuster, R. Tip-Enhanced Raman Scattering: Influence of the Tip-Surface Geometry on Optical Resonance and Enhancement. *Surf. Sci.* **2009**, *603*, 1335–1341.
- (37) Mooradian, A. Photoluminescence of Metals. *Phys. Rev. Lett.* **1969**, *22*, 185–187.
- (38) Lin, K.; Yi, J.; Zhong, J.; Hu, S.; Liu, B.; Liu, J.; Zong, C.; Lei, Z.; Wang, X.; Aizpurua, J.; *et al.* Plasmonic Photoluminescence for Recovering Native Chemical Information from Surface-Enhanced Raman Scattering. *Nat. Commun.* **2017**, *8*, 14891.
- (39) Merlen, A.; Gadenne, V.; Romann, J.; Chevallier, V.; Patrone, L.; Valmalette, J. C. Surface Enhanced Raman Spectroscopy of Organic Molecules Deposited on Gold Sputtered Substrates. *Nanotechnology* **2009**, *20*, 215705.
- (40) Berweger, S.; Neacsu, C. C.; Mao, Y.; Zhou, H.; Wong, S. S.; Raschke, M. B. Optical Nanocrystallography with Tip-Enhanced Phonon Raman Spectroscopy. *Nat. Nanotechnol.* **2009**, *4*, 496–499.